Earth Syst. Dynam. Discuss., 3, 259–278, 2012
www.earth-syst-dynam-discuss.net/3/259/2012/
doi:10.5194/esdd-3-259-2012

Earth System Dynamics Discussions

Enhanced Atlantic subpolar gyre variability through baroclinic threshold in a Coarse Resolution Model

M. Mengel[1,2], **A. Levermann**[1,2], **C.-F. Schleussner**[1,2], **and A. Born**[3,4]

[1]Potsdam Institute for Climate Impact Research, Telegrafenberg A62, 14473 Potsdam, Germany
[2]Physics Institute, Potsdam University, Potsdam, Germany
[3]Climate and Environmental Physics, Physics Institute, University of Bern, Bern, Switzerland
[4]Oeschger Centre for Climate Change Research, Bern, Switzerland

Received: 6 March 2012 – Accepted: 2 April 2012 – Published: 13 April 2012

Correspondence to: M. Mengel (mengel@pik-potsdam.de)

Published by Copernicus Publications on behalf of the European Geosciences Union.

Abstract

Direct observations, satellite measurements and paleorecords reveal strong variability in the Atlantic subpolar gyre on various time scales. Here we show that variations of comparable amplitude can only be simulated in a coupled climate model in the proximity of a dynamical threshold. The threshold and the associated dynamic response is due to a positive feedback involving increased salt transport in the subpolar gyre and enhanced deep convection in its center. A series of sensitivity experiments is performed with a coarse resolution ocean general circulation model coupled to a statistical-dynamical atmosphere model which in itself does not produce atmospheric variability. To simulate the impact of atmospheric variability, the model system is perturbed with freshwater forcing of varying but small amplitude and multidecadal to centennial periodicity, and observational variations in wind stress. While both freshwater and wind-stress-forcing have a small direct effect on the strength of the subpolar gyre, the magnitude of the gyre's response is strongly increased in the vicinity of the threshold. Our results thus indicate that baroclinic self-amplification in the North Atlantic ocean can play an important role in presently observed SPG variability and thereby North Atlantic climate variability on multidecadal scales.

1 Introduction

Most northern deep water formation occurs in the Nordic Seas in combination with strong overflows down the Greenland-Scotland ridge (GSR) and associated entrainment of surrounding water masses (Hansen et al., 2004). This deep water formation is a crucial part of the Atlantic Meridional Overturning Circulation, an important element of the global climate system. Simulations with a high resolution ocean model suggest that the Atlantic inflow into the Nordic Seas is modulated significantly by the strength of the subpolar gyre (SPG) south of the GSR (Hátún et al., 2005). Surface wind stress has strong influence on strength and variability of the SPG and the gyre strength has

ESDD
3, 259–278, 2012

been linked to the main mode of wind stress variability, the North Atlantic Oscillation (NAO) (Curry et al., 1998; Böning et al., 2006) and the Antlantic Multidecadal Oscillation (AMO) (Häkkinen et al., 2011a,b). However, part of the gyre circulation is controlled by baroclinic adjustments and thereby the density structure in the region (Greatbatch et al., 1991; Myers et al., 1996; Penduff et al., 2000; Eden and Willebrand, 2001).

Current diverging trends of NAO and SPG transport suggest that the classical picture of an NAO driven gyre is incomplete. Häkkinen et al. (2011a,b) argue that the frequency of atmospheric blocking and associated SLP anomalies in the eastern North Atlantic more closely resemble variations in the SPG. A decoupling due to baroclinic effects is discussed by Hátún et al. (2009) and Lohmann et al. (2009). Direct measurements reveal a strong freshening of the region during the last four decades of the 20th century (Reverdin, 2010; Yashayaev, 2007; Häkkinen and Rhines, 2009; Curry and Mauritzen, 2005; Dickson et al., 2002; Blindheim et al., 2000) with a reversal towards higher salinities in the Eastern North Atlantic after 2001 (Häkkinen et al., 2011a). Satellite observation of sea surface elevation suggest a rapid reduction in SPG strength between 1992 and 2003 (Häkkinen and Rhines, 2004).

Observations, higher-resolution models and fully coupled climate models with atmospheric variability exhibit strong variations of the SPG. Interannual variability can reach up to 25 % of the long-term mean and variability on multi-decadal time-scales can be even stronger (Treguier et al., 2005; Hátún et al., 2005; Häkkinen and Rhines, 2009; Böning et al., 2006). However, due to their complexity the dynamical cause of the variability is often difficult to identify in these models.

In order to understand the SPG's past role in climate variability (Born and Levermann, 2010; Thornalley et al., 2009) and to project its future evolution, the gap between simulations on short timescales with high spatial resolution and those on long timescales and lower resolution needs to be overcome. The coarse-resolution climate model CLIMBER-3α, which we apply in this study, exhibits a threshold behavior of the Atlantic SPG with respect to surface freshwater forcing (Fig. 1) that has been related to baroclinic feedbacks in the region (Levermann and Born, 2007; Born and Mignot,

ESDD
3, 259–278, 2012

2011). Similar abrupt changes in Labrador Sea convection and the SPG have been observed in a number of models of varying complexity (LeGrande and Schmidt, 2008; Wu and Wood, 2008; Jongma et al., 2007; Weijer, 2002; Born et al., 2011) as well as sea surface temperature and sea ice reconstructions over the last 140 yr (Dima and Lohmann, 2011). The cessation of Labrador Sea convection and a subsequent weakening of the SPG is a prominent feature in 21st century global warming simulations with AOGCMS (Yin et al., 2010; Landerer et al., 2007).

The appreciation of the SPG's non-linear and feedback driven dynamics has proven useful for the understanding of historic climate events. The existence or lack of an overflow over the GSR, for example, can change the baroclinic response of the SPG to surface wind-stress forcing and may have led to qualitatively different behavior in glacial and interglacial periods (Montoya et al., 2010). Paleoclimatic time series in the North Atlantic suggest that a transition of the SPG from a predominantely weak to a strong state has occurred during the so-called 8.2 ka event at the beginning of the present interglacial (Born and Levermann, 2010) when a meltwater outburst from North American proglacial lakes weakened the Atlantic overturning circulation and led to widespread cooling over Europe. Furthermore, the SPG likely delayed the last glaciation over Scandinavia by controlling the Atlantic inflow into the Nordic Seas (Born et al., 2010, 2011).

After a brief description of model and experiments, we present the threshold behavior for the SPG under stationary preindustrial boundary conditions exhibiting two distinct regimes. By analysis of the temperature and salinity fields we identify three feedback loops that lead to the non-linear response of the SPG through self-amplification in our model. We propose that this self-amplification plays a crucial role in multidecadal gyre variability, as illustrated by the SPG response to time-dependent variations in surface freshwater flux and wind-stress as a function of the distance from the threshold.

ESDD
3, 259–278, 2012

2 Model and experiments

The coupled climate model CLIMBER-3α applied in this study comprises interactive atmosphere, sea ice and ocean components (Montoya et al., 2005). The oceanic general circulation model is based on the GFDL MOM-3 code (Pacanowski and Griffies, 1999), with 24 variably spaced vertical levels, a coarse horizontal resolution of 3.75°, a background vertical diffusivity of $\kappa_h = 0.3 \times 10^{-4}\,m^2\,s^{-1}$ and an eddy-induced tracer advection with a thickness diffusion coefficient of $\kappa_{gm} = 250\,m^2\,s^{-1}$. If not denoted differently wind stress is prescribed to climatology (Trenberth et al., 1989). We apply an improved version of the model used in Levermann and Born (2007) that exhibits a more realistic strength of the meridional overturning circulation. The statistical-dynamical atmosphere model (Petoukhov et al., 2000) does not produce internal variability. We explore this shortcoming using three sets of experiments: (1) equilibrium simulations with constant anomalous surface freshwater forcing, (2) sinosoidal freshwater forcing in addition to the constant forcing of (1), and (3) time-varying surface wind stress reanalysis forcing in addition to (1). Anomalous surface freshwater flux is applied between 63.75–78.75° N and 11.25° W–10° E in the Nordic Seas. It leads to fresher surface waters and increased sea ice cover which remotely acts on the gyre dynamics through reduced overturning in the Nordic Seas. Note that no freshwater forcing is applied on the convection sites south of the Greenland Scotland Ridge and thereby no direct influence on the SPG is induced. We will show here that the remote forcing, however, induces strong shifts in the SPG dynamics.

In (1) we look at the equilibrium response after at least 1000 yr of integration with constant freshwater forcing. In (2) sinusoidal variations are added to the experiments of (1) in the same geographical region after equilibration. Amplitudes are varied between 5 and 30 mSv ($1\,mSv = 10^3\,m^3\,s^{-1}$) and periods are 25 to 200 yr. In (3) surface wind stress anomalies from the NCEP-NCAR reanalysis (Kalnay et al., 1996) were added to the climatology (Trenberth et al., 1989). Anomalies were computed as the annual mean minus the average over the full period from 1948 to 2009. In order to avoid drifts

ESDD
3, 259–278, 2012

and discontinuities, the anomalies time series from 1948–2009 is continued by its time-reversed time series. The resulting 122-yr-long time series is cyclic and is used as a long-term representation of presently observed variability. In order to be able to let the simulation run into a dynamic equilibrium this forcing is repeated several times.

3 SPG threshold behaviour and mechanism of transition

In response to a constant surface freshwater forcing we identify a threshold behavior with two distinct regimes of circulation (Fig. 1). Within the explored forcing interval between ±200 mSv (inlay in Fig. 1) we find a sharp increase of 40 % (from 20 Sv to 28 Sv) in SPG volume transport, measured as the maximum absolute value of the horizontal streamfunction in the gyre region, at 15 mSv anomalous freshwater forcing. This intensification of the transport is in geostrophic balance with the density changes in the gyre. Consequently, the stronger gyre is associated with an enhanced density difference between its denser center and the relatively light outer rim of the gyre. This finding has been discussed in detail by Levermann and Born (2007).

The strong circulation regime is characterized by a cooler SPG center and a warmer northern rim (Fig. 2a and b). Surface salinities are higher along the path of waters entrained from the North Atlantic Current (NAC) at the northern part of the gyre (Fig. 2c and d) with positive anomalies extending into the SPG center. The density increase over the whole upper 1000 m in the center (Fig. 2e and f) is, however, dominated by lower temperatures (compare to Fig. 2a and b). The cooling, freshening and density increase at the southern part of the SPG reflects the southeastward shift of the NAC due to the intensification and associated spatial expansion of the SPG (Fig. 2h). This expansion has been observed in periods of enhanced SPG volume transport in the Atlantic (Bersch et al., 2007; Häkkinen and Rhines, 2009; Häkkinen et al., 2011a). A prominent feature of the strong circulation is the additional southern region of winter convection at the SPG center (Fig. 2, gray rectangles). The heat flux to the atmosphere increases over the northern SPG region (Fig. 2g) and ensures that the additional heat

ESDD
3, 259–278, 2012

that is entrained together with tropical NAC waters is released to the atmosphere in such a way that there is a net cooling in the center of the SPG. The strong negative heat flux anomaly at the southern SPG rim is due to a southward shift of the NAC.

Since we find a threshold behaviour in equilibrium simulations, this nonlinearity has to be associated with positive feedbacks within the system. We argue that three feedback loops sustain the strong circulation once it has been initiated (Fig. 3). First, the strong SPG entrains more warm and saline tropical NAC waters into the gyre (Levermann and Born, 2007; Born and Mignot, 2011). This increases the surface salinity and weakens the stratification in the subpolar region, which fosters winter convection and heat loss to the atmosphere at the SPG center. The resulting cooler center temperatures increase the density contrast between center and rim and thus geostrophic SPG transport (loop 1). The stronger entrainment leads to a warming of the outer rim waters which decreases their density and thus adds to the center-rim density contrast and geostrophic SPG transport (loop 2). The stronger SPG is associated with a southeastward extension of the gyre and a longer path for entrained waters until they reach the core of the SPG. This causes a higher cumulative heat loss on the path which contributes further to the observed cooler temperatures in the SPG center, thus increases the density contrast and geostrophic SPG transport (loop 3).

Even though our coarse resolution model fails to represent North Atlantic ocean-atmosphere dynamics in their full complexity, the mechanism reported here is consistent with the relation between the cessation of subpolar deep convection in the late 1990s and a slowing down and westward contraction (Bersch et al., 2007; Häkkinen and Rhines, 2004, 2009; Häkkinen et al., 2011a) of the SPG which is speculated to be induced by internal dynamics (Lohmann et al., 2009).

We diagnose the Atlantic Meridional Overturning Circulation (AMOC) to be 6.5 % weaker in the strong circulation regime in our model. While this out-of-phase behaviour opposes some model results (Böning et al., 2006), it is consistent with observations (Zhang, 2008) and other model findings (Zhang, 2008; Manabe and Stouffer, 1999).

ESDD
3, 259–278, 2012

4 Role of threshold for SPG variability

In order to investigate the role of the threshold behavior for SPG variability we introduced temporal variations in surface freshwater and wind stress forcing (Fig. 4). In the standard simulation, i.e. without a constant off-set in freshwater forcing and thereby far away from the threshold, the application of the observed wind stress anomalies results in relatively weak SPG variability of less than 2 Sv. Similarly low variability is obtained for sinusoidal surface freshwater flux variations with 20 mSv amplitude and a period of 100 yr.

The SPG response drastically increases when the system is brought closer to the threshold by application of a constant freshwater flux off-set. In this case both forcings induce a high SPG variability of 10 Sv for wind-stress and 15 Sv for sinusiodal freshwater forcing, respectively. Similar values were obtained from satellite sea surface observations (Häkkinen and Rhines, 2004, 2009) and model results (Böning et al., 2006) yielding 10 Sv or 25 % transport variability.

Spatial patterns of variability for temperature, salinity and density mimic the anomaly patterns from baroclinic feedbacks we discussed in the previous chapter. Thus, the increase of variability originates from the feedback driven dynamical regime in our model. The high correlation of center temperature, center density and SPG strength in Fig. 4 supports this finding. Salinity plays an important role in modulating convection but does not drive density changes directly, it is anticorrelated with density in the upper 1000 m average.

The robustness of the variability increase is detailed in Fig. 5 where SPG mean and standard deviation are plotted over the respective freshwater flux off-set. Different colors correspond to different forcing amplitudes of the sinusoidal freshwater flux. The qualitative behavior is best seen for a forcing amplitude of 100 yr: SPG variability shows an abrupt increase at an off-set similar to the threshold for constant freshwater forcing of 15 mSv. Variability decreases when we move away from the threshold towards higher offsets. The increase of mean and variability are not tightly linked. Variability is

ESDD
3, 259–278, 2012

high for runs near the threshold because the SPG meanders between the two equilibrium states. Mean strength monotonically increases with higher offsets, analogous to the equilibrium simulations. This particular feature illustrates the dynamic core of the variability. Though the transition of the time-dependent behavior reflects the equilibrium threshold of Fig. 1, it is not equivalent to the equilibrium response but reflects a dynamical behaviour as expressed in the variance. The dynamical transition occurs over a large interval of forcing amplitudes and is largely independent of this forcing amplitude.

The same behavior although less pronounced is found for shorter forcing periods of 25 and 200 yr (Fig. 6). For reanalysis surface wind stress forcing (Fig. 5, lower panels) we observe a similar behaviour. SPG variability is relatively constant at a low level as long as the SPG is too far from the threshold. At the threshold of 15 mSv of constant freshwater off-set the amplitude of the time-varying response increases and stays strong beyond the threshold.

5 Conclusion and discussion

Here we present simulations with a coarse-resolution climate model to better understand the mechanisms of SPG variability. In equilibrium, the SPG exhibits a threshold behavior with respect to surface freshwater flux which results from positive baroclinic feedbacks within the subpolar region. It is important to note that the freshwater is not applied on the SPG but north of the Greenland Scotland Ridge. The SPG response is thereby induced by circulation changes through baroclinic feedbacks. This non-linear behavior enhances SPG variability drastically for variations in surface freshwater forcing with a magnitude comparable to observed changes in precipitation in the region.

Wind-stress forcing from reanalysis data only produces gyre transport variability similar to observations if the system is brought close to the threshold. The observed high variability of SPG transport may thus indicate a near-threshold gyre circulation. A near-threshold gyre circulation might collapse into a permanent weak SPG circulation as found in model simulations under global warming scenarios (Yin et al., 2009).

ESDD
3, 259–278, 2012

While it is clear that our results are not directly applicable to presently observed variability on interannual time scales, they suggest a potential role of the associated baroclinic feedbacks on multi-decadal time scales. In fact, the abrupt weakening of the SPG during the 1990s has been associated with similar processes as responsible for our results (Häkkinen and Rhines, 2004). In our simulation the SPG already responds to forcing of 25-yr period, but pronounced variability is found for periods of 50 yr and longer. The effect increases with the length of the period due to the long SPG response time in the model. The response time is set by the baroclinic adjustment and may not be accurately captured at coarse resolution. A general problem of coarse resolution models is a possible dilution of temperature and salinity signals due to the large grid boxes. We thus hypothesize that the time scales in our model might be larger than they would be at higher resolution. In that case strong variability of shorter period than 50 yr might be possible.

Though the threshold behavior of Labrador Sea convection has been reported for a number of models of varying complexity (Legrande et al., 2006; Wu and Wood, 2008; Born et al., 2011), we can not rule out that it is due to the coarseness of the model or due to deficiencies in the density structure produced by the model. Analyses of higher resolution models with and without atmospheric variability are necessary to investigate the robustness of our results.

Acknowledgements. This research was supported by the German Environmental Foundation (DBU) and the German National Academic Foundation. A. B. is supported by the "National Centre for Excellence in Research: Climate" of the Swiss National Science Foundation.

ESDD
3, 259–278, 2012

References

Bersch, M., Yashayaev, I., and Koltermann, K. P.: Recent changes of the thermohaline circulation in the subpolar North Atlantic, Ocean Dynam., 57, 223–235, 2007. 264, 265

Blindheim, J., Borovkov, V., Hansen, B., Malmberg, S.-A., Turrell, W. R., and Osterhus, S.: Upper layer cooling and freshening in the Norwegian Sea in relation to atmospheric forcing, Deep-Sea Res. Pt. I, 47, 655–680, 2000. 261

Böning, C. W., Scheinert, M., Dengg, J., Biastoch, A., and Funk, A.: Decadal variability of subpolar gyre transport and its reverberation in the North Atlantic overturning, Geophys. Res. Lett., 33, L21S01, doi:10.1029/2006GL026906, 2006. 261, 265, 266

Born, A. and Levermann, A.: The 8k event: abrupt transition of the subpolar gyre towards a modern North Atlantic circulation, Geochem. Geophy. Geosy., 11, 1361–1371, 2010. 261, 262

Born, A. and Mignot, J.: Dynamics of decadal variability in the Atlantic subpolar gyre: a stochastically forced oscillator, Clim. Dynam., doi:10.1007/s00382-011-1180-4, in press, 2011. 261, 265

Born, A., Nisancioglu, K., and Braconnot, P.: Sea ice induced changes in ocean circulation during the Eemian, Clim. Dynam., 35, 1361–1371, 2010. 262

Born, A., Nisancioglu, K., and Risebrobakken, B.: Late Eemian warming in the Nordic Seas as seen in proxy data and climate models, Paleoceanography, 26, PA2207, doi:10.1029/2010PA002027, 2011. 262, 268

Curry, R. and Mauritzen, C.: Dilution of the Northern North Atlantic Ocean in Recent Decades, Science, 308, 1772–1774, 2005. 261

Curry, R. G., McCartney, M. S., and Joyce, T. M.: Oceanic transport of subpolar climate signals to mid-depth subtropical waters, Nature, 391, 575–577, 1998. 261

Dickson, B., Yashayaev, I., Meincke, J., Turrell, B., Dye, S., and Holfort, J. T.: Rapid freshening of the deep North Altantic Ocean over the past four decades, Nature, 416, 832–837, 2002. 261

Dima, M. and Lohmann, G.: Hysteresis Behavior of the Atlantic Ocean Circulation identified in Observational Data, J. Climate, 24, 397–403, 2011. 262

Eden, C. and Willebrand, J.: Mechanism of Interannual to Decadal Variability of the North Atlantic Circulation, J. Climate, 14, 2266–2280, 2001. 261

ESDD
3, 259–278, 2012

Greatbatch, R. J., Fanning, A. F., Goulding, A. D., and Levitus, S.: A diagnosis of interpentadal circulation changes in the North Atlantic, J. Geophys. Res., 96, 22009–22023, 1991. 261
Häkkinen, S. and Rhines, P. B.: Decline of Subpolar North Atlantic Circulation During the 1990s, Science, 304, 555–559, 2004. 261, 265, 266, 268
Häkkinen, S. and Rhines, P. B.: Shifting surface currents in the northern North Atlantic Ocean, J. Geophys. Res., 114, C04005, doi:10.1029/2008JC004883, 2009. 261, 264, 265, 266
Häkkinen, S., Rhines, P., and Worthen, D.: Warm and saline events embedded in the meridional circulation of the northern North Atlantic, J. Geophys. Res.-Ocean., 116, 3006, doi:10.1029/2010JC006275, 2011a. 261, 264, 265
Häkkinen, S., Rhines, P., and Worthen, D.: Atmospheric Blocking and Atlantic Multidecadal Ocean Variability, Science, 334, 655–659, doi:10.1126/science.1205683, 2011b. 261
Hansen, B., Ø sterhus, S., Quadfasel, D., and Turrell, W.: Already the Day After Tomorrow?, Science, 305, 953–954, 2004. 260
Hátún, H., Sandø, A. B., Drange, H., Hansen, B., and Valdimarsson, H.: Influence of the Atlantic Subpolar Gyre on the Thermohaline Circulation, Science, 309, 1841–1844, 2005. 260, 261
Hátún, H., Payne, M., Beaugrand, G., Reid, P., Sandø, A., Drange, H., Hansen, B., Jacobsen, J., and Bloch, D.: Large bio-geographical shifts in the north-eastern Atlantic Ocean: From the subpolar gyre, via plankton, to blue whiting and pilot whales, Prog. Oceanogr., 80, 149–162, 2009. 261
Jongma, J., Prange, M., Renssen, H., and Schulz, M.: Amplification of Holocene multicentennial climate forcing by mode transitions in North Atlantic overturning circulation, 34, L15706, doi:10.1029/2007GL030642, 2007. 262
Kalnay, E., Kanamitsu, M., Kistler, R., Collins, W., Deaven, D., Gandin, L., Iredell, M., Saha, S., White, G., Woollen, J., Zhu, Y., Chelliah, M., Ebisuzaki, W., Higgins, W., Janowiak, J., Mo, K. C., Ropelewski, C., Wang, J., Leetmaa, A., Reynolds, R., Jenne, R., and Joseph, D.: The NCEP/NCAR 40-Year Reanalysis Project, B. Am. Meteorol. Soc., 77, 437–471, 1996. 263
Landerer, F. W., Jungclaus, J. H., and Marotzke, J.: Regional Dynamic and Steric Sea Level Change in Response to the IPCC-A1B Scenario, J. Phys. Oceanogr., 37, 296–312, 2007. 262
LeGrande, A. and Schmidt, G.: Ensemble, water isotope-enabled, coupled general circulation modeling insights into the 8.2 ka event, Paleoceanography, 23, PA3207, doi:10.1029/2008PA001610, 2008. 262

ESDD
3, 259–278, 2012

Legrande, A., Schmidt, G., Shindell, D., Field, C., Miller, R., Koch, D., Faluvegi, G., and Hoffmann, G.: Consistent simulations of multiple proxy responses to an abrupt climate change event, P. Natl. Acad. Sci., 103, 837–842, 2006. 268

Levermann, A. and Born, A.: Bistability of the subpolar gyre in a coarse resolution climate model, Geophys. Res. Lett., 34, L24605, doi:10.1029/2007GL031732, 2007. 261, 263, 264, 265

Lohmann, K., Drange, H., and Bentsen, M.: A possible mechanism for the strong weakening of the North Atlantic subpolar gyre in the mid-1990s, 36, L15602, doi:10.1029/2009GL039166, 2009. 261, 265

Manabe, S. and Stouffer, R.: The rôle of thermohaline circulation in climate, Tellus A, 51, 91–109, 1999. 265

Montoya, M., Griesel, A., Levermann, A., Mignot, J., Hofmann, M., Ganopolski, A., and Rahmstorf, S.: The Earth System Model of Intermediate Complexity CLIM*BER*-3α, Part I: description and performance for present day conditions, Clim. Dynam., 25, 237–263, 2005. 263

Montoya, M., Born, A., and Levermann, A.: Reversed North Atlantic gyre dynamics in present and glacial climates, Clim. Dynam., 1107–1118, doi:10.1007/s00382-009-0729-y, 2010. 262

Myers, P. G., Fanning, A. F., and Weaver, A. J.: Jebar, bottom pressure torque, and gulf stream separation, J. Phys. Oceanogr., 26, 671–683, 1996. 261

Pacanowski, R. C. and Griffies, S. M.: The MOM-3 manual, Tech. Rep. Tech. Rep. 4, NOAA/Geophyical Fluid Dynamics Laboratory, Princeton, NJ, USA, 1999. 263

Penduff, T., Barnier, B., and de Verdière, A. C.: Self-adapting open boundaries for a sigma coordinate model of the eastern North Atlantic, J. Geophys. Res., 105, 279–298, 2000. 261

Petoukhov, V., Ganopolski, A., Brovkin, V., Claussen, M., Eliseev, A., Kubatzki, C., and Rahmstorf, S.: CLIMBER-2: a climate system model of intermediate complexity, Part I: model description and performance for present climate, Clim. Dynam., 16, 1–17, 2000. 263

Reverdin, G.: North Atlantic subpolar gyre surface variability (1895–2009), J. Climate, 23, 4571–4584, 2010. 261

Rodwell, M., Rowell, D., and Folland, C.: Oceanic forcing of the wintertime North Atlantic Oscillation and European climate, Nature, 398, 320–323, 1999.

Thornalley, D., Elderfield, H., and McCave, I.: Holocene oscillations in temperature and salinity of the surface subpolar North Atlantic, Nature, 457, 711–714, doi:10.1038/nature07717, 2009. 261

ESDD
3, 259–278, 2012

Treguier, A. M., Theetten, S., Chassignet, E. P., Penduff, T., Smith, R., Talley, L., Beismann, J. O., and Böning, C.: The North Atlantic Subpolar Gyre in Four High-Resolution Models, J. Climate, 35, 757–774, 2005. 261

Trenberth, K., Olson, J., and Large, W.: A Global Ocean Wind Stress Climatology based on ECMWF Analyses, Tech. Rep. NCAR/TN-338+STR, National Center for Atmospheric Research, Boulder, Colorado, USA, 1989. 263

Weijer, W.: Response of the Atlantic overturning circulation to South Atlantic sources of buoyancy, Global Planet. Change, 34, 293–311, 2002. 262

Wu, P. and Wood, R.: Convection induced long term freshening of the subpolar North Atlantic Ocean, Clim. Dynam., 31, 941–956, 2008. 262, 268

Yashayaev, I.: Hydrographic changes in the Labrador Sea, 1960–2005, Prog. Oceanogr., 73, 242–276, 2007. 261

Yin, J., Schlesinger, M. E., and Stouffer, R. J.: Model projections of rapid sea-level rise on the northeast coast of the United States, Nat. Geosci., 2, 262–266, 2009. 267

Yin, J., Griffies, S., and Stouffer, R.: Spatial Variability of Sea Level Rise in Twenty-First Century Projections, J. Climate, 23, 4585–4607, 2010. 262

Yoshimori, M., Raible, C., Stocker, T., and Renold, M.: Simulated decadal oscillations of the Atlantic meridional overturning circulation in a cold climate state, Clim. Dynam., 34, 101–121, 2010.

Zhang, R.: Coherent surface-subsurface fingerprint of the Atlantic meridional overturning circulation, Geophys. Res. Lett., 35, L20705, doi:10.1029/2008GL035463, 2008. 265

ESDD
3, 259–278, 2012

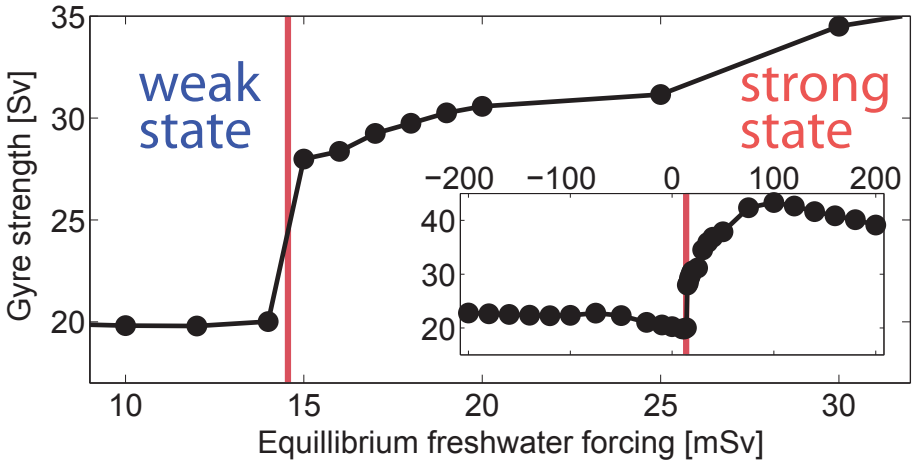

Fig. 1. Equilibrium threshold behavior of Atlantic SPG volume transport in response to constant surface freshwater flux. The SPG exhibits a threshold behavior at 15 mSv forcing strength where it intensifies by more than 40 %. The inlay shows its response in the entire forcing interval of ±200 mSv.

ESDD
3, 259–278, 2012

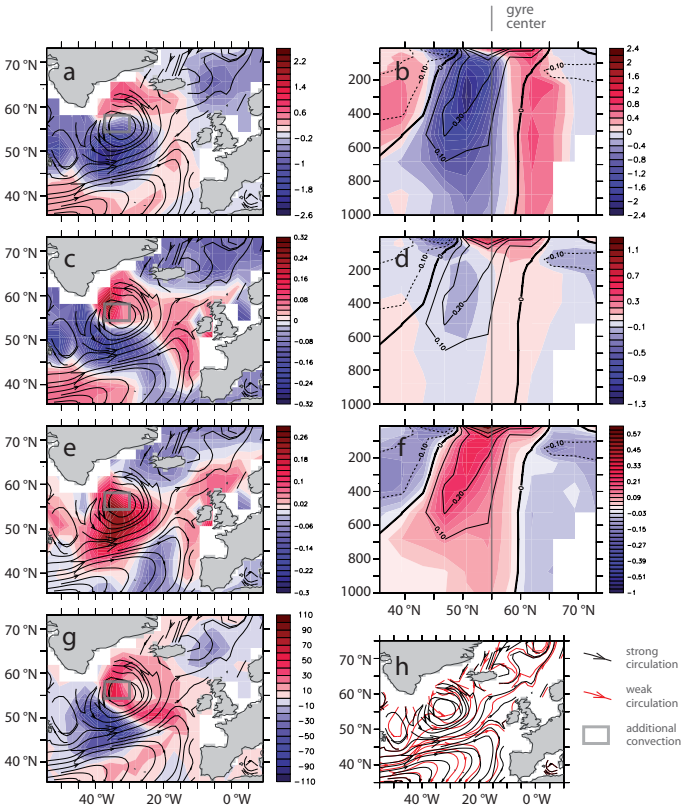

Fig. 2. Difference between the strong (15 mSv forcing) and weak (control) SPG circulation. Panels **(a, b)** show temperature, **(c, d)** salinity, **(e, f)** density and **(g)** heatflux. Panels **(a, c, e)** show averages over the upper 1000 m, black flowlines in panels **(a, c, e, g)** show upper 1000 m strong state velocities. Panel **(h)** compares strong (black) and weak (red) upper 1000 m velocities. Panels **(b, d, f)** show zonal averages between 37.5° and 18.75° W with density anomalies as contours and the approximate gyre center as a grey line.

ESDD
3, 259–278, 2012

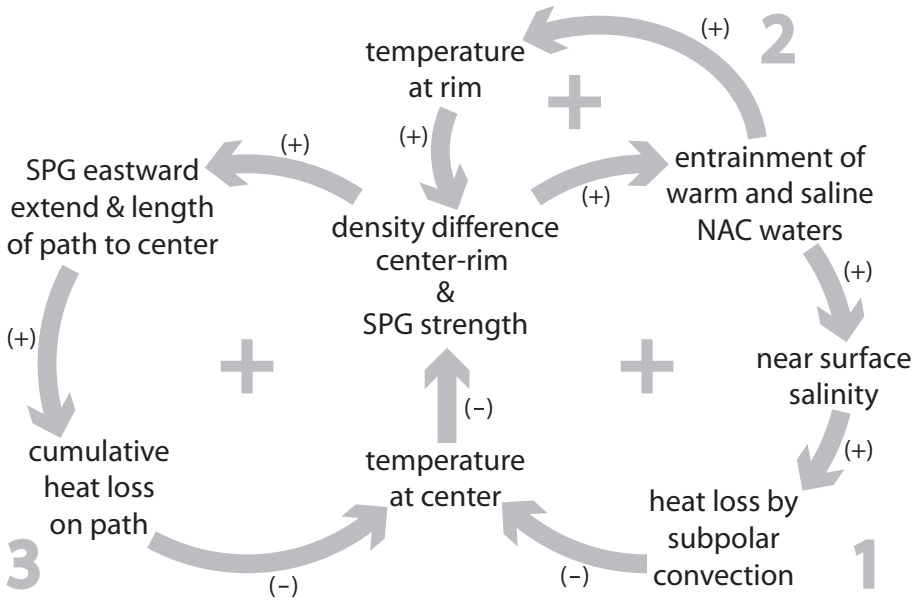

Fig. 3. Feedback loops leading to the self-amplification of the SPG transport as described in the text. The stronger SPG entrains more warm and saline North Atlantic Current water, increasing the surface salinity in the subpolar region, which fosters winter convection and thereby leads to cooler temperatures at the SPG center, increasing the center-rim density contrast and thus geostrophic SPG transport (loop 1). The stronger entrainment leads to a warming and density decrease of the rim waters, thus adds to the density contrast and geostrophic SPG transport (loop 2). The stronger SPG goes along with a southeastward extension and a longer path for entrained waters to reach the SPG core region. This causes a higher cumulative heat loss on the path which leads to cooler center temperatures, thus enhances the density difference and geostrophic SPG transport (loop 3).

ESDD
3, 259–278, 2012

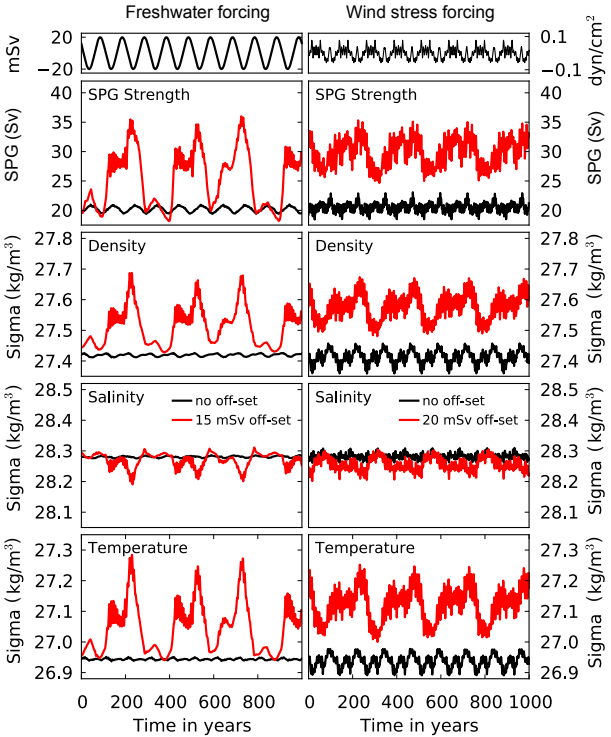

Fig. 4. Time series of SPG strength showing enhanced variability near the dynamical threshold due to baroclinic feedbacks. Upper two panels show time-varying forcing, the two panels below SPG strength. Lower three rows show: density in the center of the gyre (full density variations, changes due to salinity and changes due to temperature). Averages are taken between 37.5° W–18.75° W and 45° N–60° N in the upper 1000 m. Left column: with sinusoidal freshwater forcing of 20 mSv amplitude and a period of 100 yr. The black curves are without constant freshwater off-set while the red curves represent a 15 mSv off-set. Right column: with NCEP surface wind stress anomaly without (black curve) and with constant freshwater off-set of 20 mSv (red curve). In both cases SPG variability is significantly weaker than observed when the system is far from the threshold (black curves). In the vicinity of the dynamical threshold of Fig. 1, the SPG variability is drastically increased. The main density signal is produced by temperature variations. Major salinity changes are restricted to the surface layers, but play a key role in the process of self-amplification (see Fig. 3).

ESDD
3, 259–278, 2012

Baroclinic SPG variabilty

M. Mengel et al.

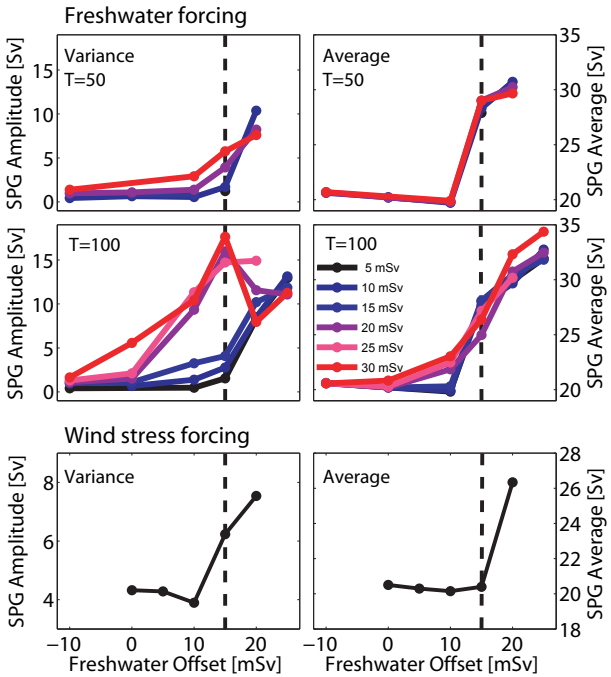

Fig. 5. Upper and middle panels: mean SPG strength and its variability for different constant off-set in surface freshwater flux. Different lines correspond to the forcing amplitudes as denoted in the legend. Lower panels: Wind induced variability of the SPG for different constant freshwater off-sets. The dashed vertical line marks the position of the equilibrium threshold at 15 mSv (compare to Fig. 1). The amplitude of SPG variations increases when approaching the threshold for both time-varying freshwater and wind stress forcing. This is best seen for the 100 yr period freshwater forcing, but still present on the shorter timescales (50 yr period and wind stress forcing). Even close to the threshold the system's response to NCEP wind stress variability is significantly smaller than its response to centennial scale freshwater variations.

ESDD
3, 259–278, 2012

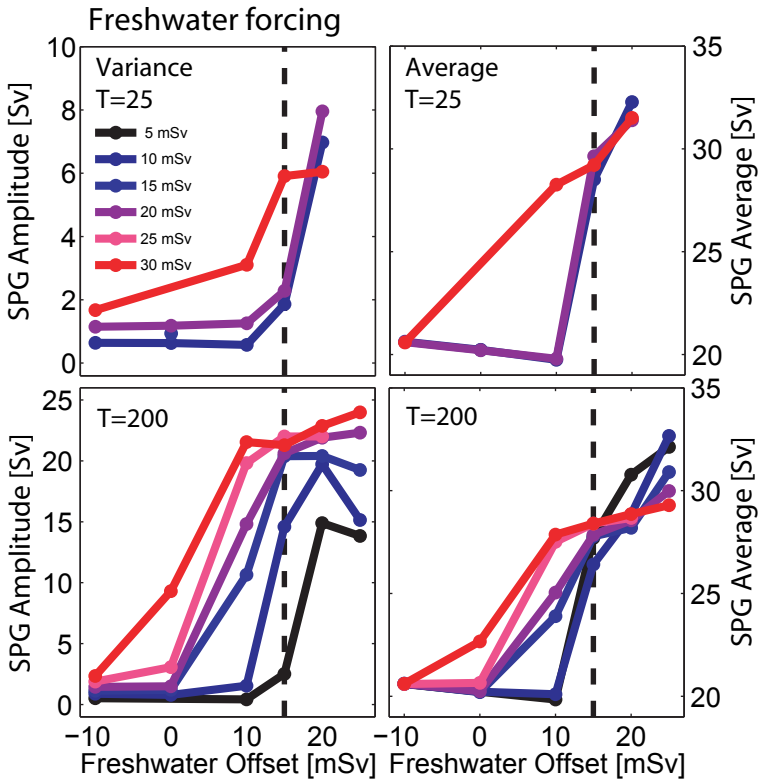

Fig. 6. Mean SPG strength and its variability for varying perturbation amplitude corresponding to Fig. 5, but for periods of 25 and 200 yr. Different lines correspond to different forcing amplitudes as denoted in the legend.

ESDD
3, 259–278, 2012